Polyhedron 50 (2013) 51–58

Contents lists available at SciVerse ScienceDirect

Polyhedron

journal homepage: www.elsevier.com/locate/poly

Synthesis, crystal structure and DFT analysis of a phenoxo bridged Cu(II) complex and an azide and μ_3-O mixed bridged trinuclear Cu(II) complex

Sangita Ray [a], Saugata Konar [a], Atanu Jana [a], Kinsuk Das [b], Ray J. Butcher [c], Tapan Kumar Mondal [d], Susanta Kumar Kar [a,*]

[a] Department of Chemistry, University College of Science, University of Calcutta, 92, A.P.C. Road, Kolkata 700009, India
[b] Department of Chemistry, Haldia Government College, Debhog, Purba Midnapur 721657, India
[c] Department of Chemistry, Howard University, 2400 Sixth Street, N.W., Washington, DC 200 59, USA
[d] Department of Chemistry, Jadavpur University, Kolkata 700032, India

A R T I C L E I N F O

Article history:
Received 21 April 2012
Accepted 16 September 2012
Available online 2 November 2012

Keywords:
Copper (II) complexes
Pyrimidine derived Schiff base ligands
Spectral properties
X-ray crystal structures
DFT

A B S T R A C T

One binuclear Cu(II) complex, $[Cu_2(L_1)_2(N_3)_2]$ (**1**), and a trinuclear Cu(II) complex, $[Cu_3(L_2)_3(\mu_{1,1}\text{-}N_3)_2](ClO_4)$ (**2**), of two potentially tridentate NNO-donor Schiff base ligands, [2-(1-(2-(4,6-dimethylpyrimidin-2-yl)hydrazono)ethyl)phenol] (HL_1) and [2-((2-(4,6-dimethyl pyrimidin-2-yl) hydrazono) methyl) phenol] (HL_2), have been synthesized and characterized by elemental analyses, UV–Vis IR spectroscopy, DFT and single crystal X-ray crystallography. The ligands HL_1 and HL_2 are [1 + 1] condensation products of 2-hydrazino-4,6-dimethylpyrimidine with 2-hydroxy acetophenone and salicylaldehyde respectively. In **1**, the two Cu(II) centers are bridged by μ-phenoxo groups. In **2**, the three Cu(II) centers are held together by two $\mu_{1,1}$ bridging azide ions and a phenoxo oxygen atom which binds the three metal centers and behaves as a μ_3-O atom. The geometries of the complexes have been optimized using the UB3LYP level of theory. The calculation confirms that all the copper centers are five coordinate with distorted square pyramidal geometries, which is consistent with the experimental data.

1. Introduction

In recent decades, much attention has been paid to synthesizing copper(II) trinuclear [1,2] and binuclear [3,4] complexes. Polydentate Schiff base ligands have preparative accessibility, structural variety and varied denticity, forming complexes of different coordination numbers and nuclearities with interesting molecular and crystalline architectures [5–7]. A substantial amount of work on pyridine and pyrazole derived Schiff base ligands has emerged in the literature, while works on pyrimidine derived Schiff base ligands are scarce. Pyrimidine derived metal ion complexes have been extensively studied in recent years owing to their great variety of biological activity, ranging from antimalarial, antibacterial, antitumoral, antiviral activities, etc. [8–13], which have often been related to their chelating ability with trace metal ions. Nucleic acids, vitamins and co-enzymes containing pyrimidine ring systems provide potential binding sites for metal ions. The higher π acidity and the presence of more than one hetero atom in pyrimidine play an important role in its coordination chemistry, compared to that of pyridine bases, and serve as better models in biological systems [14–16]. Trinuclear and dinuclear copper complexes have received considerable interest because of their importance as model systems for the active sites of multinuclear proteins and metalloenzymes [17–20]. Most of the reported trinuclear Cu(II) complexes have a linear geometry, whereas trinuclear non-linear Cu(II) complexes are comparatively few in number [21].

As a sequel to our long standing interest in pyrimidine derived ligands [22–24], we have prepared tridentate NNO donor Schiff base ligands using 2-hydrazino-4,6-dimethylpyrimidine, 2-hydroxy acetophenone and salicylaldehyde. In the present study (Scheme 1), using copper perchlorate as the metal precursor, one new dinuclear copper(II) complex, $[Cu_2(L_1)_2(N_3)_2]$ (**1**), and one new trinuclear copper(II) complex, $[Cu_3(L_2)_3(\mu_{1,1}\text{-}N_3)_2](ClO_4)$ (**2**), have been synthesized with HL_1 and HL_2. We have reported the synthetic details, spectral characterizations, DFT, a comparison between the calculations and the experimental data, X-ray crystal structures and electrochemical properties of **1** and **2** where the phenoxo groups, and both the $\mu_{1,1}$ azide and phenoxo groups act as bridging units respectively.

2. Experimental

2.1. Materials

All chemicals were of reagent grade, purchased from commercial sources and used without further purification. Salicylaldehyde

---

* Corresponding author. Tel.: +91 033 23508386; fax: +91 033 23519755.
E-mail address: skkar_cu@yahoo.co.in (S.K. Kar).

0277-5387/$ - see front matter © 2012 Elsevier Ltd. All rights reserved.
http://dx.doi.org/10.1016/j.poly.2012.09.061

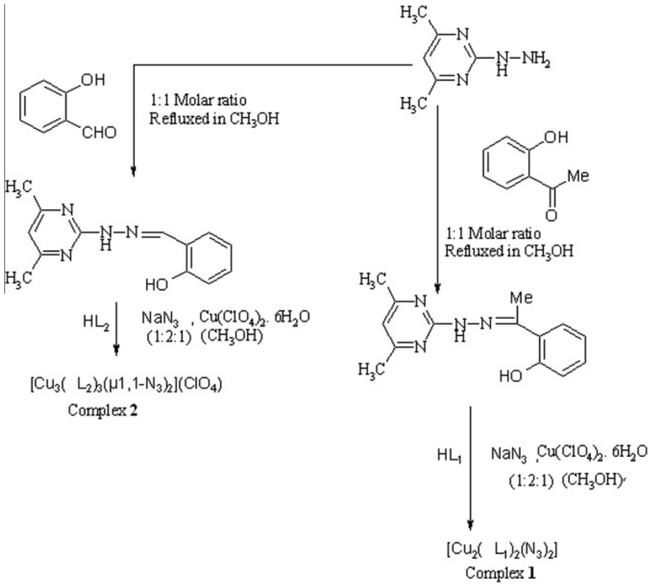

Scheme 1. Schematic representation of the ligands (HL_1 and HL_2) and their complexes.

and 2-hydroxy acetophenone were purchased from Aldrich Chemical Company, USA and used without further purification.

Caution! Although we have not encountered any problems, it should be kept in mind that sodium azide and perchlorate compounds of metal ions are potentially explosive, especially in the presence of organic ligands. Only a small amount of the material should be prepared and it should be handled with care.

2.2. Physical measurements

Elemental analyses (carbon, hydrogen and nitrogen) of the ligands and the metal complexes were determined with a Perkin–Elmer CHN analyzer 2400 at the Indian Association for the Cultivation of Science; Kolkata. The electronic spectra of the complexes in methanolic solution were recorded on a Hitachi model U-3501 spectrophotometer. IR spectra (KBr pellet, 400–4000 cm^{-1}) were recorded on a Perkin–Elmer model 883 infrared spectrophotometer. ^1H NMR spectra of the ligands were recorded in $CDCl_3$ with a Bruker AM 300L (300 MHz) superconducting FTNMR spectrometer. Cyclic voltammetry was carried out with a Sycopel model AEW2 1820F/L instrument. All electrochemical measurements were made in DMF on a BAS (Epsilon model) having a three-electrode setup consisting of glassy carbon (polished with alumina before measurement) working, platinum wire auxiliary and Ag/AgCl reference electrodes. Oxygen was rigorously removed from the DMF solutions of the samples by purging with dry argon gas of high purity.

2.3. Syntheses of the ligands HL_1 and HL_2

The ligand HL_1 was synthesized by refluxing a methanol solution (30 ml) of 2-hydrazino-4,6-dimethylpyrimidine [24,25] (1.38 g, 10 mmol), with 2-hydroxy acetophenone (1.36 g, 10 mmol) taken in the same solvent. Refluxing was continued for 1 h at water bath temperature. The resulting light yellow solution was filtered and kept at room temperature for slow evaporation. A light yellow microcrystalline compound separated out after a week. It was filtered off, washed several times with cold methanol and dried in vacuo over fused $CaCl_2$.

The ligand HL_2 was synthesized and characterized using the literature method [26].

HL_1: (Yield: 85.30%); M.p. (°C) 159; *Anal.* Calc. for $C_{14}H_{16}N_4O$: C, 65.62; H, 6.25; N, 21.80 Found: C, 65.52; H, 6.17; N, 21.40%. IR (ν, cm^{-1}): 3247 (ν_{NH}), 1620 ($\nu_{C=C}$), 1635 ($\nu_{C=NH}$), 885 (ν_{Cpym-H}), 1255 (ν_{C-O}); ^1H NMR (300 MHz, $CDCl_3$, 25 °C, TMS) δ/ppm: 6.68 (s,1H, C_5–H pyrimidine), 6.8–7.3 (m, 4H, Pym ring), 8.2 (s,1H, –CH=N–), 12.8 (s, 1H, aromatic –OH), 2.28 (s,1H, N–H of hydrazone), 2.46–2.53 (m, 6H, CH_3).

2.4. Preparation of the complexes

2.4.1. Preparation of complex **1**

To a methanolic solution (30 ml) of $Cu(ClO_4)_2{\cdot}6H_2O$ (0.370 g, 2 mmol), a solution of the Schiff base HL_1 (0.512 g, 2 mmol) was added, followed by a solution of sodium azide (0.260 g, 4 mmol) in a minimum volume of methanol with constant stirring for 2 h. This mixture was kept at room temperature, yielding green hexagonal crystals suitable for X-ray diffraction after 10 days. The crystals were isolated by filtration and air-dried. (Yield: 65.5%). *Anal.* Calc. for $C_{30}H_{30}Cu_2N_{14}O_4$: C, 46.20; H, 3.85; N, 25.1. Found: C, 46.10; H, 3.81; N, 24.89%. IR (KBr; ν/cm^{-1}): 2065 (vs) (ν_{as}, N_3^-), 1619 (s) ($\nu_{c=Npym}$). UV–Vis (MeOH) λ_{max}/nm: 386 and 607.

2.4.2. Preparation of complex 2

To a methanolic solution (30 ml) of $Cu(ClO_4)_2{\cdot}6H_2O$ (0.370 g, 2 mmol), a solution of the Schiff base HL_2 (0.484 g, 2 mmol) was added, followed by a solution of sodium azide (0.260 g, 4 mmol) in a minimum volume of methanol with constant stirring for 2 h. This mixture was kept at room temperature, yielding green hexagonal crystals suitable for X-ray diffraction after 10 days. The crystals were isolated by filtration and air-dried. (Yield: 61.7%). *Anal.* Calc. for $C_{41}H_{45}Cu_3ClN_{18}O_9$: C, 42.4; H, 3.87; N, 21.7 Found: C, 42.3; H, 3.77; N, 21.30%. IR (KBr; ν/cm^{-1}): 625(s) and 1100 (s, br) (uncoordinated perchlorate), 2069 (vs) (ν_{as}, N_3^-), 1610 (s) ($\nu_{c=Npym}$), UV–Vis (MeOH) λ_{max}/nm: 400 and 612.

2.5. Single crystal X-ray crystallography

Crystal data for the two complexes are given in Table 1. Data were collected with Mo Kα radiation, for **1** using a Bruker-AXS SMART APEX II diffractometer and for **2** using an Oxford Diffraction X-Calibur CCD System. Absorption corrections were carried out using the SADABS program [27]. Data analysis was carried out with the CRYSALIS program [28]. Both structures were solved using direct methods with the SHELXS97 program [29]. An empirical absorption correction for **2** was carried out using the ABSPACK program [30]. The structures were refined on F^2 using SHELXL97 [29].

2.6. Computational methods

Full geometry optimizations of complexes **1** and **2** have been carried out in the UB3LYP [31–33] level DFT computational method in triplet ($S = 1$) and quartet ($S = 3/2$) states respectively using the GAUSSIAN 03 software package [34]. For C, H, N and O atoms, the 6–31+G(d) basis set was assigned, while for Cu the LANL2DZ basis set with an effective core potential was employed [35]. Vibrational frequency calculations were performed to ensure that the optimized geometries represent the local minima and there are only positive Eigen values. Vertical electronic excitations based on optimized geometries were computed for the time-dependent density functional theory (TD-DFT) formalism [36–38] in MeOH using the conductor-like polarizable continuum model (CPCM) [39–41]. Gauss Sum [42] was used to calculate the fractional contributions of the various groups to each molecular orbital.

Table 1
Experimental data for crystallographic analyses of **1** and **2**.

Compound	**1**	**2**
Formula	$C_{30}H_{38}Cu_2N_{14}O_4$	$C_{41}H_{45}ClCu_3N_{18}O_9$
Formula weight	785.84	1160.02
T (K)	150	295
λ (Å)	0.71073	1.54178
Crystal system	monoclinic	monoclinic
Space group	*C*2/*c*	*P*2$_1$/*m*
Unit cell dimensions		
a (Å)	20.463(2)	11.1763(1)
b (Å)	9.8220(8)	18.9296(2)
c (Å)	18.1022(18)	11.7307(1)
α (°)	90	90
β (°)	110.565(5)	98.773(1)
γ (°)	90	90
V (Å^3)	3406.5(6)	2452.75(4)
Z	4	2
Density$_{cal}$ (Mg m^{-3})	1.532	1.571
Absorption coefficient (mm^{-1})	1.307	2.627
F(000)	1624	1186
Crystal size (mm^3)	0.11 × 0.13 × 0.14	0.12 × 0.32 × 0.48
θ Range (°) for data collection	2.1–28.4	4.5–77.5
Index ranges	$-27 \leqslant h \leqslant 27$ $-12 \leqslant k \leqslant 13$ $-22 \leqslant l \leqslant 24$	$-14 \leqslant h \leqslant 13$ $-23 \leqslant k \leqslant 15$ $-14 \leqslant l \leqslant 14$
Goodness-of-fit on F^2	1.027	1.062
Completeness to theta = 25.00° (%)	98.3	99.9
Independent reflections (R_{int})	4222 (R_{int} = 0.0650)	5288 (R_{int} = 0.0156)
Absorption correction	multi-scan	multi-scan
Refinement method	full-matrix least squares on F^2	full-matrix least squares on F^2
Reflections collected	21549	11195
Final *R* indices [$I > 2\sigma(I)$]	R_1 = 0.0444 WR_2 = 0.1294	R_1 = 0.0483 WR_2 = 0.1348
Largest difference peak and hole (e Å^{-3})	−0.68, 0.38	−0.965, 0.989

3. Result and discussion

3.1. Syntheses

The ligands HL_1 and HL_2 were synthesized by the direct condensation reactions of 2-hydrazino-4,6-dimethylpyrimidine with 2-hydroxy acetophenone and salicylaldehyde respectively, taken in methanol in a 1:1 mol proportion. The complexation behavior of HL_1 and HL_2 towards Cu(II) perchlorate was investigated. Complexes **1** and **2** were obtained by mixing the ligands, Cu(II) perchlorate and sodium azide, taken in a 1:1:2 molar ratio in methanol. X-ray quality crystals of **1** and **2** were obtained upon slow evaporation of the reaction mixtures at room temperature.

3.2. Structural description of complex 1

A perspective view of complex **1** with the atom numbering scheme is shown in Fig. 1. Selected metrical parameters are given in Table 1. Complex **1** crystallizes in the space group *C*2/*c*. The structure of $[Cu_2(L_1)_2(N_3)_2]$ (**1**) is a non-centrosymmetric dimer, as shown in Fig. 1, with each metal atom in a five-coordinate environment. The unit cell of **1** comprises of four molecules. The Addison parameter (τ) of the pentacoordinate Cu(II) is 0.314, suggesting the predominance of a square-based pyramidal (SP) geometry. The metal atom is bonded to the uninegative tridentate ligand L_1 via O1 at 1.870(2), N1 at 1.972(2) and N3 at 2.002(3) Å, together with a bridging oxygen atom O1_a from a second ligand at 2.751(2) Å and a terminal azide ion *via* N5 at 1.964(3) Å. The two Cu atoms are separated by 3.371 Å and the Cu1–O1–Cu1_a angle is 91.64°. The copper(II) ion is 0.111 Å above the basal plane. The crystal structure of these compounds can be described as a 1D layer due to intermolecular hydrogen bonding. A 3D view of complex **1**, with trapped water molecules within chains is shown in Fig. 2. The structure is stabilized by a network of intermolecular hydrogen bonding, H3AB of N3A and O1 of CH_3OH and H1 of CH_3OH and N4A of pyrimidine (Fig. 3). Details of the hydrogen bonding are given in Table 3.

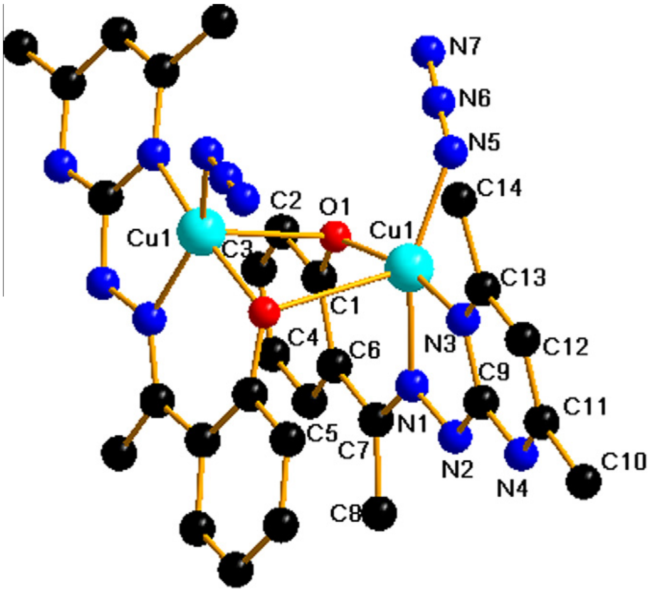

Fig. 1. Structural representation and atom numbering scheme of **1** (H-atoms are omitted for clarity).

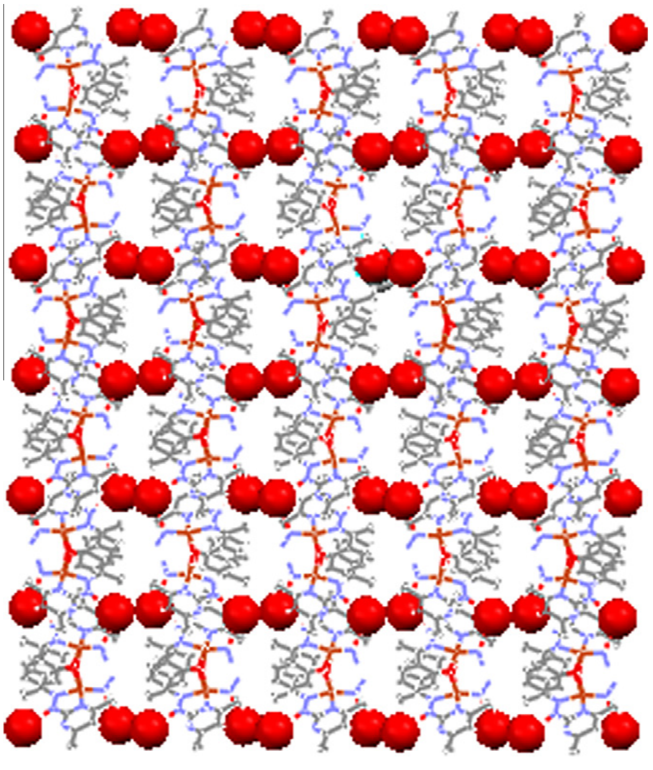

Fig. 2. 3D view of complex **1** with trapped methanol molecules within the chains.

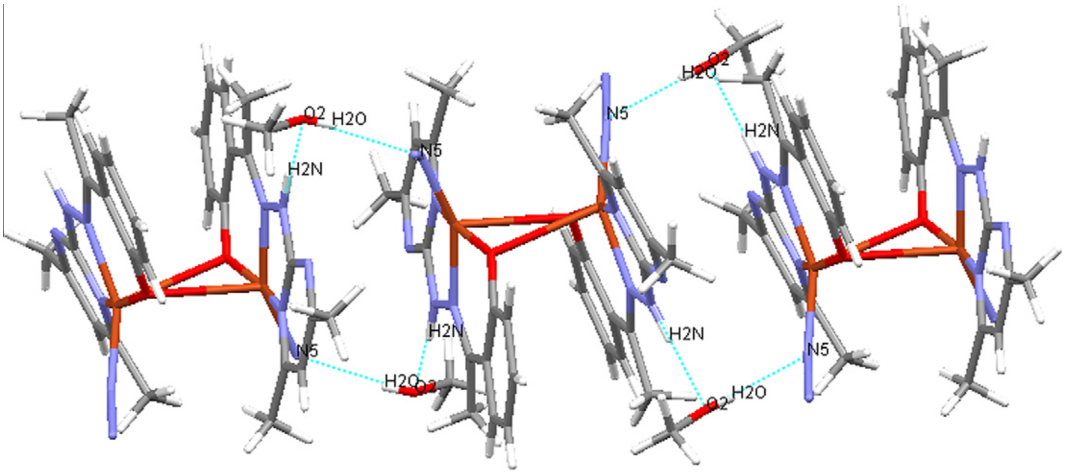

Fig. 3. Hydrogen bonding interactions in complex **1**.

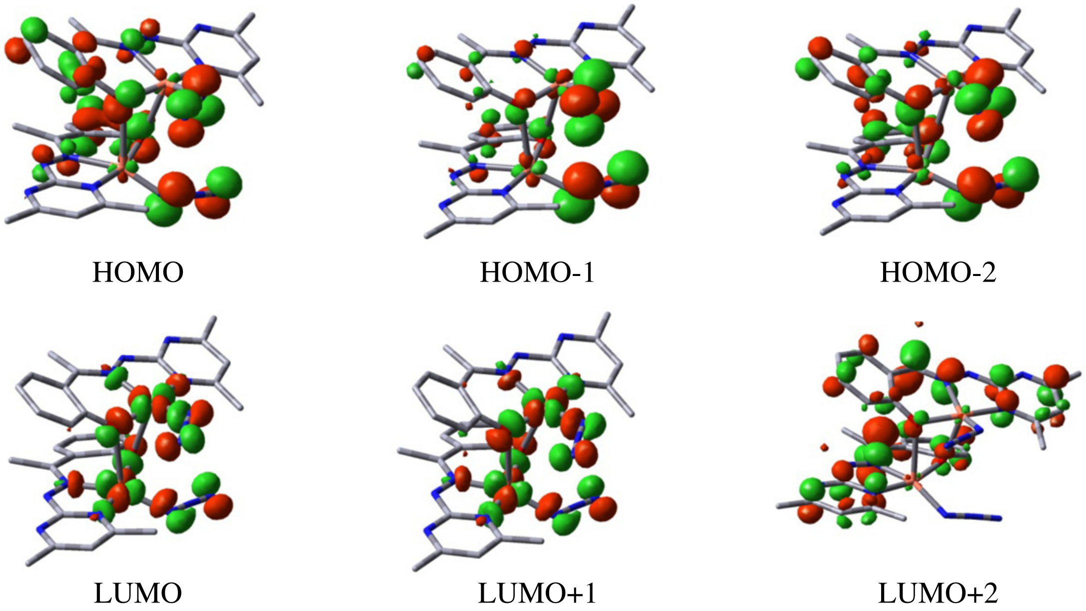

Fig. 4. Contour plots of some selected MOs (β-spin) of **1**.

3.3. Structural description of complex **2**

A perspective view of complex **2** with the atom numbering scheme is shown in Fig. 5. Selected metrical parameters are given in Table 2. Complex **2** crystallizes in the space group $P2_1/m$ and its unit cell comprises of two molecules. The structure consists of two distinct entities of $[Cu(L_2)_2]$ and $[Cu(L_2)]$, where two identical $Cu(L_2)_2$ units and a CuL_2 unit are bridged by two $\mu_{1,1}$-azido groups and a μ_3-phenoxo oxygen atom. The geometry of the two identical terminal Cu(II) centers are best described as distorted square pyramidal with a N_3O_2 chromophore (τ = 0.099). The basal plane of Cu1 is occupied by O1A from a phenoxo group, N1A from azomethine, N2A from pyrimidine, N11 from a bridging azide, and the apical position by the oxygen atom O1B from another ligand molecule (Cu1–N1A 1.937, Cu1–N2A 2.034, Cu1–N11 1.983, Cu1–O1B 2.79 Å). The central Cu(II) center has a trigonal bipyramidal geometry with a N_4O chromophore, τ = 0.95 [31]. The trigonal plane is formed by two N11 atoms from two different bridging azides and one azomethine, N1B. The apical positions are occupied by N2B pyrimidine and O1B phenoxo oxygen atoms of the ligand molecule. The O1B atom is a μ_3-phenoxo oxygen, acting as a three connecting node in the structure (Cu2–N1B 1.961, Cu2–N2B 1.999, Cu2–O1B 1.899, Cu2–N11 2.162 Å). The Cu1–Cu2–Cu1 angle is 113.21°, Cu(1)–N(11)–Cu(2) is 104.15° and Cu(1)–O(1B)–Cu(2) is 86.15°. The Cu1 center is 0.03 Å above the mean plane. The 3D view of complex **2** with trapped perchlorate molecules within the chains is shown in Fig. 6. The structure is stabilized by a network of intermolecular hydrogen bonding, H3AB of pyrimidine and O1 of CH_3OH, and H1 of CH_3OH and N4A of pyrimidine (Fig. 7). Details of the hydrogen bonding are given in Table 3.

3.4. DFT calculations and electronic structure

The geometry optimizations of complexes **1** and **2** were carried out using the (U) B3LYP/DFT method, taking the coordinates of their respective X-ray structures. The calculated bond parameters well reproduced the experimental structures with minor deviations (Table 2). The α-spin occupied and virtual orbitals have HL_1 and HL_2

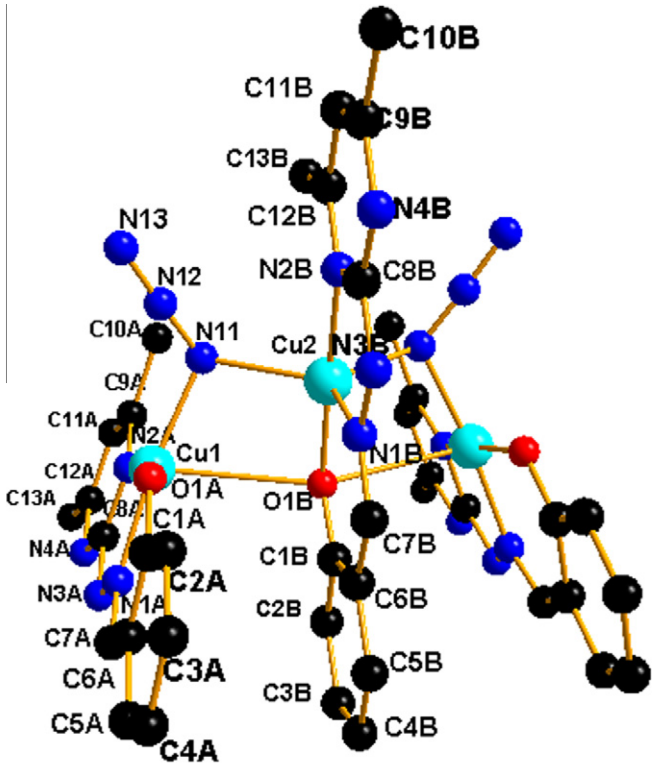

Fig. 5. Structural representation and atom numbering scheme of **2** (H-atoms are omitted for clarity).

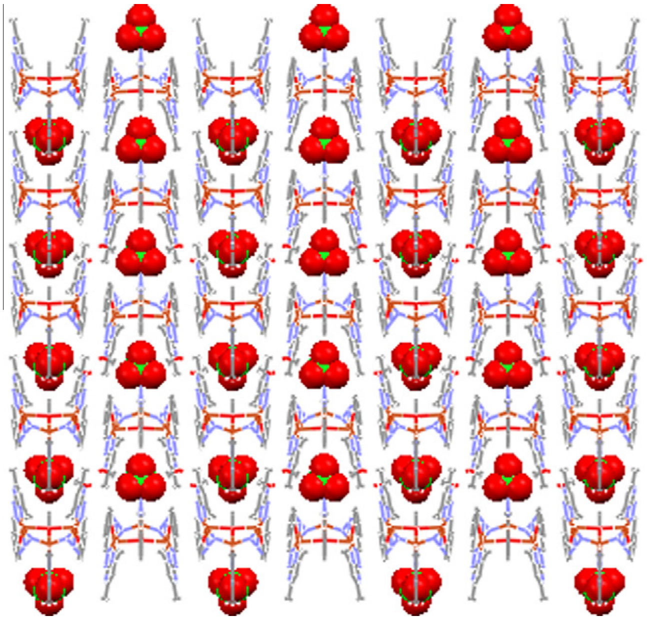

Fig. 6. 3D view of complex **2** with trapped methanol molecules within the chains.

characters in **1** and **2** respectively, along with a contribution of N_3^- in the occupied orbitals (Tables 6 and 7 in the supplementary materials). The β-spin LUMO and LUMO + 1 have 50% Cu(dπ) in complex **1**, while LUMO to LUMO + 2 in complex **2** have 53–61% Cu(dπ)

Table 2
Selected bond distances (Å) and angles (°) in **1** and **2**.

Selected bonds	(Å)	Calculated value (Å)	Selected angles	(°)	Calculated value (°)
Complex **1**					
Cu1–O1	1.870(2)	1.936	N1–Cu1–N3	82.60(9)	80.17
Cu1–N5	1.964(3)	1.960	N1–Cu1–N5	155.22(12)	154.2
Cu1–N1	1.972(2)	2.037	Cu1–O1–Cu1_a	91.64(9)	92.72
Cu1–N3	2.002(3)	2.116	O1–Cu1–N1	91.52(10)	89.56
Cu1–O1_a	2.751(2)	2.657	O1–Cu1–N3	164.98(10)	164.3
			O1–Cu1–N5	91.47(11)	92.88
			O1–Cu1–O1_a	83.71(9)	81.08
			O1_a–Cu1–N1	86.31(8)	87.44
			N3–Cu1–N5	99.67(11)	100.6
			O1_a–Cu1–N3	82.13(9)	87.99
			O1_a–Cu1–N5	118.47(10)	118.3
			Cu1–O1–Cu1_a	91.64(9)	92.72
			Cu1–N1–N2	110.99(15)	110.6
			Cu1–N5–N6	120.3(3)	120.0
Complex **2**					
Cu1–O1A	1.895(2)	1.928	O1A–Cu1–O1B	89.31(9)	92.42
Cu1–O1B	2.7939(8)	2.790	O1A–Cu1–N1A	91.26(9)	90.60
Cu1–N1A	1.937(2)	1.992	O1A–Cu1–N2A	166.85(10)	166.6
Cu1–N2A	2.043(2)	2.101	O1A–Cu1–N11	87.30(9)	88.88
Cu1–N11	1.983(2)	2.003	O1B–Cu1–N1A	101.82(9)	99.09
Cu2–O1B	1.899(3)	1.949	O1B–Cu1–N2A	102.84(8)	101.6
Cu2–N1B	1.961(3)	2.028	O1B–Cu1–N11	71.14(9)	72.57
Cu2–N2B	1.999(3)	2.064	N1A–Cu1–N2A	81.44(9)	79.74
Cu2–N11	2.162(2)	2.186	N1A–Cu1–N11	172.82(10)	171.5
Cu2–N11_b	2.162(2)	2.186	N2A–Cu1–N11	101.27(9)	103.0
			O1B–Cu2–N1B	92.72(14)	91.14
			O1B–Cu2–N2B	174.23(14)	171.2
			O1B–Cu2–N11	89.13(8)	89.15
			N1B–Cu2–N2B	81.51(14)	80.11
			N1B–Cu2–N11	121.50(6)	123.5
			Cu1–O1B–Cu1_b	155.63(13)	153.4
			Cu1–N1A–N3A	113.51(17)	112.9
			Cu2–N1B–N3B	112.4(2)	111.4
			Cu1–N11–N12	116.5(2)	115.1
			Cu2–N11–N12	117.14(19)	117.4
			Cu1–N11–Cu2	104.15(10)	102.8

Table 3
Details of hydrogen bond distances (Å) and angles (°) for **1** and **2**.

D–H...A	d(D–H)	d(H...A)	d(D...A)	<(DHA)
Complex **1**				
N2--H2N..O2	0.8800	2.0300	2.879(4)	161.00
O2 --H2O..N5	0.67(3)	2.23(4)	2.891(5)	169(5)
Complex **2**				
O1--H1..N4A	0.8200	2.1400	2.928(4)	162.00
N3A--H3AB..O1	0.8600	1.8700	2.718(4)	167.00
N3B--H3BB..O11	0.8600	2.0100	2.874(6)	176.00

Symmetry transformations used to generate equivalent atoms:
For **1** *a* = [2756.00] = 2 − *x*, *y*, 3/2 – *z*.
For **2** *a* = [4565.00] = *x*, 3/2 − *y*, *z*; *b* = [4565.00] = *x*, 3/2 − *y*, *z*.

character (Figs. 4 and 8). Other low-lying virtual orbitals have HL_1 (π^*)/L_2(π^*) contributions. The β-spin HOMO to HOMO-5 orbitals have L_1/N_3^- character for **1** with a reduced, 16–17%, Cu(dπ) contribution in HOMO-4 and HOMO-5. The β-spin HOMO to HOMO-10 have L_2 and/or N_3^- character, with only 10–13% contribution of Cu(dπ) are in HOMO-6 and HOMO-8 (Tables 8 and 9 in the supplementary materials). In both the complexes the β-spin occupied orbitals mainly take part in electronic transitions.

3.5. Electronic spectra

The electronic solution spectra of the complexes were recorded in MeOH solution. The spectra of the Cu(II) complexes **1** and **2** exhibit a strong band at 386 and 400 nm, along with very weak low-intensity absorption bands at 607 and 612 nm, respectively. To assign the electronic transitions corresponding to these bands, TDDFT calculations on the optimized geometries of **1** and **2** have been performed in methanol. The TDDFT results show low energy weak transitions corresponding to $HL_1(\pi)/N_3^- \rightarrow$ Cu(dπ) in complex **1** and $HL_2(\pi) \rightarrow$ Cu(dπ) transitions in complex **2**. The intense bands at 386 and 400 nm for **1** and **2** respectively correspond to $HL(\pi) \rightarrow HL(\pi^*)$ transitions, along with a reduced contribution of $N_3^- \rightarrow HL(\pi^*)$ (Tables 4 and 5). The electronic spectrum of the free ligand HL_1 shows a band at 345 nm attributed to the $n \rightarrow \pi^*$ transition of the azomethine group. There is a strong band at 280 nm due to a $\pi \rightarrow \pi^*$ transition.

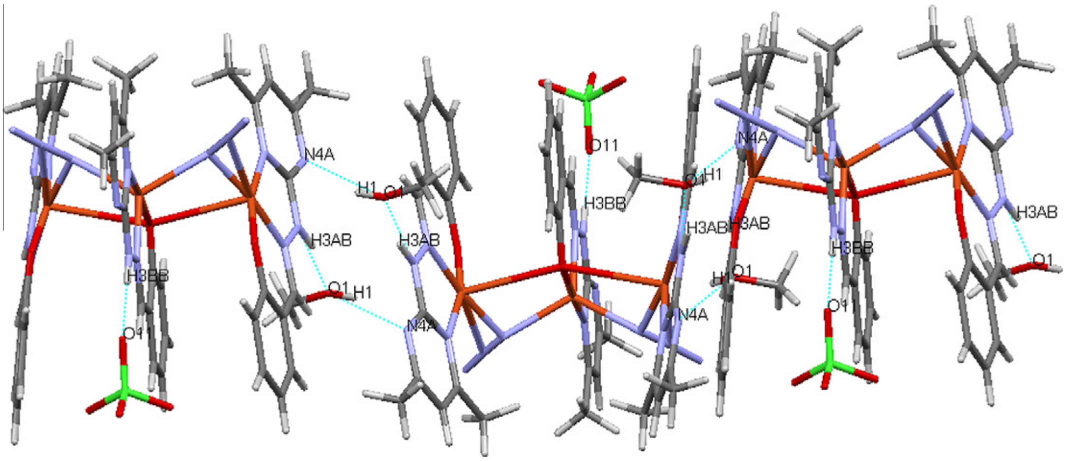

Fig. 7. Hydrogen bonding interactions in complex **2**.

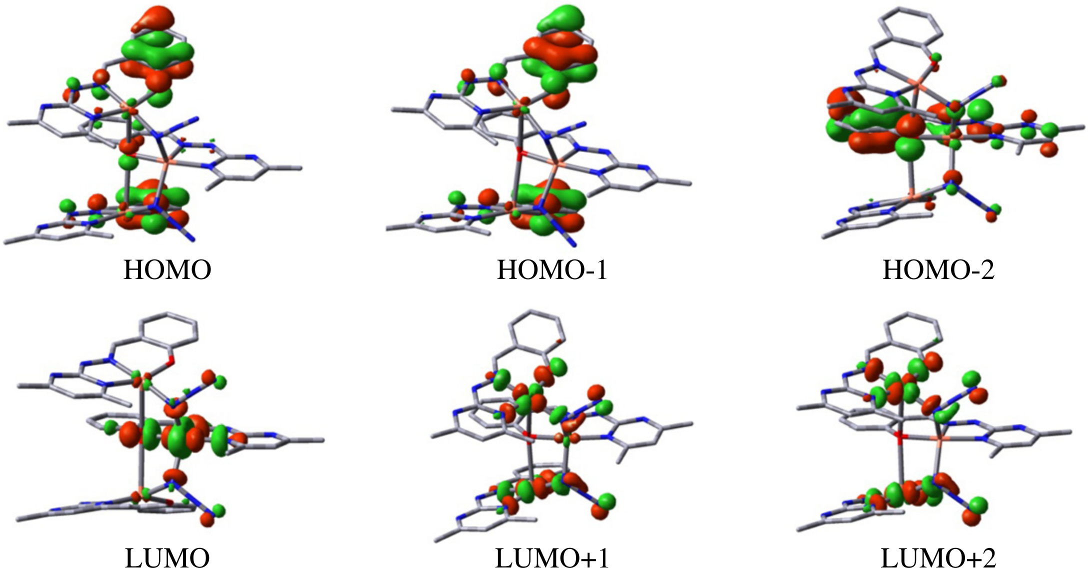

Fig. 8. Contour plots of some selected MOs (β-spin) of **2**.

Table 4
Selected vertical excitations calculated by the TDDFT method for **1**.

$E_{excitation}$ (eV)	$\lambda_{excitation}$ (nm)	Osc. strength (f)	Key transition	Character	$\lambda_{expt.}$ (nm)
1.7904	692.5	0.0257	(37%)HOMO-2(β) → LUMO(β) (35%)HOMO-3(β) → LUMO(β)	$L_1(\pi)/N_3^- \rightarrow Cu(d\pi)$	
1.9223	645.0	0.0134	(42%)HOMO-1(β) → LUMO(β) (31%)HOMO-1(β) → LUMO+1(β)	$L_1(\pi)/N_3^- \rightarrow Cu(d\pi)$	607
2.5917	478.4	0.0652	(43%)HOMO-3(β) → LUMO+1(β) (27%)HOMO-2(β) → LUMO+1(β)	$L_1(\pi)/N_3^- \rightarrow Cu(d\pi)$	
3.0453	407.1	0.1552	(47%)HOMO(α) → LUMO(α) (35%)HOMO-1(β) → LUMO+2(β)	$L_1(\pi)/N_3^- \rightarrow L_1(\pi^*)$	386
3.8335	323.4	0.0956	(42%)HOMO-6(β) → LUMO+2(β) (30%)HOMO-7(β) → LUMO+2(β)	$L_1(\pi) \rightarrow L_1(\pi^*)$	
4.1727	297.1	0.1762	(67%)HOMO-6(α) → LUMO(α)	$L_1(\pi) \rightarrow L_1(\pi^*)$	

Table 5
Selected vertical excitations calculated by the TDDFT method for **2**.

$E_{excitation}$ (eV)	$\lambda_{excitation}$ (nm)	Osc. strength (f)	Key transition	Character	$\lambda_{expt.}$ (nm)
1.6885	734.3	0.0074	(51%)HOMO-2(β) → LUMO+1(β) (23%)HOMO-3(β) → LUMO+1(β)	$L_2(\pi) \rightarrow Cu(d\pi)$	
2.0707	598.8	0.0123	(57%)HOMO-1(β) → LUMO(β) (31%)HOMO-1(β) → LUMO+1(β)	$L_2(\pi) \rightarrow Cu(d\pi)$	612
2.3324	531.6	0.0153	(59%)HOMO-5(β) → LUMO(β)	$L_2(\pi) \rightarrow Cu(d\pi)$	
2.8653	432.7	0.0577	(43%)HOMO-4(β) → LUMO+3(β) (27%)HOMO-5(β) → LUMO+3(β)	$L_2(\pi) \rightarrow L(\pi^*)$	400
3.1215	397.2	0.1105	(39%)HOMO-8(β) → LUMO+3(β) (33%)HOMO-9(β) → LUMO+3(β)	$L_2(\pi)/N_3^- \rightarrow L(\pi^*)$	

3.6. Electrochemistry

The study of the electrochemical behavior of complex **2** was carried out in the positive range. Fig. 9 displays a representative cyclic voltammogram of **2**. The complex **2** exhibits a irreversible reduction peak ($E_{1/2}$) in DMF solution near +0.55 V versus SCE due to the Cu(II)/Cu(I) couple and the ΔE_{pa} value of 143 mV suggests a irreversible one electron process.

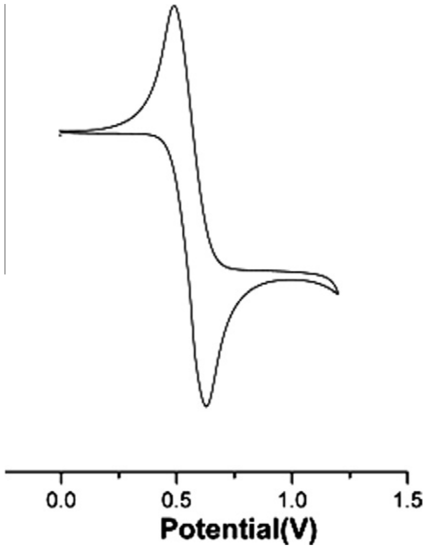

Fig. 9. Cyclic voltammogram of complex **2**.

3.7. Infrared spectroscopy

The infrared spectra of the complexes are consistent with the structural data given in this paper. The band at 2030 cm^{-1} for **1** is attributed to the terminal azide (N_3^-) group, while a strong sharp peak at 2069 cm^{-1} for **2** is assigned as the $\mu_{1,1}$ azide bridge [43,44]. The strong $\nu_{C=N}$ bands occurring at 1619 and 1610 cm^{-1} for **1** and **2** respectively are shifted considerably towards lower frequencies compared to that of the free Schiff base ligand (1635 cm^{-1}), indicating coordination of the imino nitrogen atom [45]. In **2**, the presence of a very broad band at ca. 1100 cm^{-1} (from 1050 to 1150 cm^{-1}) and a sharp one at 625 cm^{-1} indicates that the perchlorate ion still has T_d symmetry and is not, therefore, coordinated to the metal ion.

4. Conclusion

Pyrimidine based tridentate ligands HL_1 and HL_2 have been used to synthesize a binuclear Cu(II) complex (**1**) and a trinuclear Cu(II) complex (**2**), with Cu(II) perchlorate as the metal salt and using azide as a bridging ligand. The ligand HL_1 forms a binuclear phenoxo bridged neutral complex with terminal azide ligands, but the ligand HL_2 forms a trinuclear complex in which two types of bridging have been observed. In **2**, the two terminal CuL_2 centers are connected to the central CuL_2 center by two $\mu_{1,1}$ bridging azides and a μ_3-phenoxo oxygen. Each Cu(II) center contains a ligand molecule and the phenoxo oxygen atom of the ligand take part in bonding. The phenoxo oxygen atom of the ligand molecule becomes the μ_3-oxygen, O1B, binding the central Cu(II) center by bridges to the two terminal Cu(II) centers, producing a TBP geometry around the metal ion. This interesting fact is because of the plasticity of the Cu(II) geometry, which forces the bonding atoms around the metal center to utilize their variable bonding modes.

Acknowledgements

Sangita Ray acknowledges the University Grants Commission (UGC), New Delhi, India for financial assistance. Financial support [Sanc. No. F.5-1/2007(BSR)/5-16/2007(BSR), dated 12.02.2006] from the Department of Science & Technology (DST), New Delhi, India, is also gratefully acknowledged.

Appendix A. Supplementary data

CCDC 866724 and 866725 contain the supplementary crystallographic data for **1** and **2**. These data can be obtained free of charge via http://www.ccdc.cam.ac.uk/conts/retrieving.html, or from the

Cambridge Crystallographic Data Centre, 12 Union Road, Cambridge CB2 1EZ, UK; fax: (+44) 1223-336-033; or e-mail: deposit@ccdc.cam.ac.uk. Supplementary data associated with this article can be found, in the online version, at http://dx.doi.org/10.1016/j.poly.2012.09.061.

References

[1] S. Sarkar, A. Mondal, D. Chopra, J. Ribas, K.K. Rajak, Eur. J. Inorg. Chem. 45 (2006) 3510.
[2] S. Thakurta, J. Chakraborty, G. Rosair, J. Tercero, Inorg. Chem. 47 (2008) 6227.
[3] E. Ruiz, J. Cano, S. Alvarez, P. Alemany, J. Am. Chem. Soc. 120 (1998) 11122.
[4] C. Adamo, V. Barone, A. Bencini, F. Totti, I. Ciofini, Inorg. Chem. 38 (1999) 1996.
[5] P. Comba, P.W. Hambley, Molecular Modelling of Inorganic and Coordination Compounds, second ed., VCH, Weinheim, 2001. pp. 161–162.
[6] M.K. Milčič, V.B. Medakovic, D.N. Sredojevic, N.O. Juranic, S.D. Zaric, Inorg. Chem. 45 (2006) 4755.
[7] Q. Ye, D.-W. Fu, H. Tian, R.-G. Xiong, P.W.H. Chen, S.D. Huang, Inorg. Chem. 47 (2008) 772.
[8] J.S. Casas, E.E. Castellans, M.D. Louce, J. Ellena, A. Sanchez, J. Sordo, C. Taboada, J. Inorg. Biochem. 11 (2006) 1858.
[9] D.X. West, A.E. Liberta, S.B. Padhye, R.C. Chilate, P.B. Sonawane, A.S. Kumbhar, R.G. Yerande, Coord. Chem. Rev. 123 (1993) 49.
[10] M.C. Rodriguez-Arguelles, S.J. Pinelli, J. Inorg. Biochem. 58 (1995) 157.
[11] J.S. Casas, M.S. Garcia-Tasende, C. Maichel-Mossmer, M.C. Rodriguez-Arguelles, A. Sanchez, J. Sordo, A. Vazquez-Lopez, S. Pinelli, P. Lunghi, R. Albertini, J. Inorg. Biochem. 62 (1996) 41.
[12] M.B. Ferrari, G.G. Fava, G. Tarasconi, R. Albertini, S. Pinelli, R. Starcich, J. Inorg. Biochem. 53 (1994) 13.
[13] U. Koch, B. Attenni, S. Malancona, S. Colarusso, I. Conte, M.D. Filippo, S. Harper, B. Pacini, C. Giomini, S. Thomas, I. Incitti, L. Tomei, R.D. Francesco, S. Altamura, V.G. Matassa, F. Narjes, J. Med. Chem. 49 (2006) 1693.
[14] F. Zamora, M. Kunsman, M. Sabat, B. Lippart, Inorg. Chem. 36 (1997) 1583.
[15] F. Jolibois, J. Cadet, A. Grand, R. Subra, N. Raga, V. Barone, J. Am. Chem. Soc. 120 (1998) 1864.
[16] A.R. Katritzky, C.W. Pees, A.J. Boulton, C. Mckillop, J. Heterocycl. Chem. 3 (1984) 57.
[17] D.J. Spira-Solomon, M. Allendorf, E.L. Solomon, J. Am. Chem. Soc. 108 (1986) 5318.
[18] P. Kyritsis, A. Messerschmidt, R. Huber, G.A. Salmon, A.G. Sykes, J. Chem. Soc., Dalton Trans. 5 (1993) 731.
[19] M. Tremdiere, T.B. Bieth, Phytochemistry 23 (1983) 501.
[20] A. Rompel, H. Fischer, K. Büldt-Karentzopoulos, D. Meiwes, F. Zippel, H.F. Nolting, C. Hermes, B. Krebs, H. Witzel, J. Inorg. Biochem. 59 (1995) 715.
[21] S. Thakurta, C. Rizzoli, R.J. Butcher, C.J. Gomez-Garcia, E. Garribba, S. Mitra, Inorg. Chim. Acta 363 (2010) 1395.
[22] S. Gupta, S. Pal, A.K. Barik, S. Roy, A. Hazra, T.N. Mandal, R.J. Butcher, S.K. Kar, Polyhedron 28 (2009) 711–720.
[23] S. Gupta, S. Pal, A. Barik, A. Hazra, S. Roy, T.N. Mandal, S.M. Peng, G.H. Lee, M.S.El. Fallah, J. Tercero, S.K. Kar, Polyhedron 27 (2008) 2519.
[24] G.M. Kosolapoff, C.H. Roy, J. Org. Chem. 26 (1961) 1895.
[25] M.P.V. Boarland, J.F.W. McOmie, R.N. Timms, J. Chem. Soc. 915 (1952) 4691.
[26] S. Roy, T.N. Mandal, A.K. Barik, S. Gupta, R.J. Butcher, M. Nethaji, S.K. Kar, Polyhedron 27 (2008) 593.
[27] SAINT, Version 6.02, SADABS, Version 2.03; Bruker AXS Inc., Madison, WI, 2002.
[28] CRYSALIS, Oxford Diffraction Ltd., Abingdon, UK, 2006.
[29] G.M. Sheldrick, Acta Crystallogr., Sect. A 64 (2008) 112.
[30] ABSPACK, Oxford Diffraction Ltd., Oxford, UK, 2005.
[31] A.D. Becke, J. Chem. Phys. 98 (1993) 5648.
[32] P.J. Stevens, J.F. Devlin, C.F. Chabalowski, M.J. Frisch, J. Phys. Chem. 98 (1994) 11623.
[33] C.T. Lee, W.T. Yang, R.G. Parr, Phys. Rev. B, 37 (1988) 785–789.
[34] M.J. Frisch, G.W. Trucks, H.B. Schlegel, G.E. Scuseria, M.A. Robb, J.R. Cheeseman, J.A. Montgomery Jr., T. Vreven, K.N. Kudin, J.C. Burant, J.M. Millam, S.S. Iyengar, J. Tomasi, V. Barone, B. Mennucci, M. Cossi, G. Scalmani, N. Rega, G.A. Petersson, H. Nakatsuji, M. Hada, M. Ehara, K. Toyota, R. Fukuda, J. Hasegawa, M. Ishida, T. Nakajima, Y. Honda, O. Kitao, H. Nakai, M. Klene, X. Li, J.E. Knox, H.P. Hratchian, J.B. Cross, V. Bakken, C. Adamo, J. Jaramillo, R. Gomperts, R.E. Stratmann, O. Yazyev, A.J. Austin, R. Cammi, C. Pomelli, J.W. Ochterski, P.Y. Ayala, K. Morokuma, G.A. Voth, P. Salvador, J.J. Dannenberg, V.G. Zakrzewski, S. Dapprich, A.D. Daniels, M.C. Strain, O. Farkas, D.K. Malick, A.D. Rabuck, K. Raghavachari, J.B. Foresman, J.V. Ortiz, Q. Cui, A.G. Baboul, S. Clifford, J. Cioslowski, B.B. Stefanov, G. Liu, A. Liashenko, P. Piskorz, I. Komaromi, R.L. Martin, D.J. Fox, T. Keith, M.A. Al-Laham, C.Y. Peng, A. Nanayakkara, M. Challacombe, P.M.W. Gill, B. Johnson, W. Chen, M.W. Wong, C. Gonzalez, J.A. Pople, GAUSSIAN 03, Revision D.01, GAUSSIAN Inc., Wallingford, CT, 2004.
[35] P.J. Hay, W.R. Wadt, J. Chem. Phys. 82 (1985) 270.
[36] R. Bauernschmitt, R. Ahlrichs, Chem. Phys. Lett. 256 (1996) 454.
[37] R.E. Stratmann, G.E. Scuseria, M.J. Frisch, J. Chem. Phys. 109 (1998) 8218.
[38] M.E. Casida, C. Jamorski, K.C. Casida, D.R. Salahub, J. Chem. Phys. 108 (1998) 4439.
[39] V. Barone, M. Cossi, J. Phys. Chem. A 102 (1998) 1995.
[40] M. Cossi, V. Barone, J. Chem. Phys. 115 (2001) 4708.
[41] M. Cossi, N. Rega, G. Scalmani, V. Barone, J. Comput. Chem. 24 (2003) 669.
[42] N.M. O'Boyle, A.L. Tenderholt, K.M. Langner, J. Comput. Chem. 29 (2008) 839.
[43] K. Nakamoto, Infrared and Raman Spectra of Inorganic and Coordination Compounds, fifth ed., Wiley, New York, 1997. pp. 59–60.
[44] P. Govindaswamy, Hemant P. Yennawar, Mohan Rao Kollipara, J. Organomet. Chem. 689 (2004) 3108.
[45] L. Xue, Q. Liu, H. Jiang, Org. Lett. 11 (2009) 3454.